Spatial and temporal characteristics of energy deposition by protons and alpha particles in silicon

A. S. Kobayashi, *Member, IEEE*, A. L. Sternberg, *Member, IEEE,*
L. W. Massengill, *Senior Member, IEEE,* R. D. Schrimpf, *Fellow, IEEE*
and R. A. Weller, *Senior Member, IEEE*

***Abstract*— We present spatial and temporal distributions of energy deposition in silicon obtained from Monte Carlo simulations with Geant4. Detailed simulations are performed for protons and alphas over a wide energy range and include contributions from discrete δ-rays and nuclear reactions. The simulation technique we employ produces physically realistic complex track structures for which the plausibility is evaluated by comparison to the LET, radial dose, and temporal characteristics described in previous works. The variability of events, including the distribution of energy deposition at varying distances from the ion track is discussed. Finally, we examine the temporal evolution of extreme events to investigate the physicality of the common assumption that energy deposition can be considered instantaneous.**

I. INTRODUCTION

Since the transistor was invented, it has undergone constant revision and upgrade. For over 50 years, researchers have continually increased the speed of transistors and integrated circuits by reducing power consumption and feature size. As these feature sizes continue to decrease into the nano-scale, an intimate understanding of the microscopic nature of an energetic ion's interaction with the matter through which it passes is essential for the design of radiation-hardened electronics.

In [1], Weller et al. demonstrated the results of combining simulations of physically realistic radiation events created using Geant4 [2,3], with the response of an MOS transistor to these events using a commercial device physics code. That proof-of-concept was part of a larger strategy to establish a new paradigm for single event prediction based on the detailed simulation of large ensembles of extreme radiation events with detailed microstructure. By contrast, current methods commonly model ion strikes as straight trajectories with total deposited energy based on LET and the expression of this energy as dispersed charge in the sensitive volume through application of ion-track models. This strategy makes it necessary to account for the probabilistic variations due to physics and geometry separately and consequently leaves room for error.

The introduction of a new approach to this problem brings with it the need to confirm our findings with well-established results. The purpose of this paper is to demonstrate that in the aggregate, ensembles of Geant4 events reproduce the total deposited energy and geometric distribution of deposited charge familiar from present usage and established theory. We will examine both the spatial characteristics of ion tracks in silicon and the distribution of total deposited energy as a function of radius.

The deposition of an ion's energy is often considered to be instantaneous for practical purposes. In particular, it is common to model energy deposition as a spatially narrow Gaussian with instantaneous energy deposition everywhere in the target for device simulations. Here we will investigate the temporal evolution of energy deposited by extreme ion strikes in silicon. Predicting the time-evolution of energy deposited by ions quantifies the assumption that ions deposit their energy instantaneously and thereby speaks to an important practical issue in combining Geant4 and device physics simulations.

There already exists a large body of work that has been developed to understand and characterize these interactions both experimentally and analytically. In [4], Howard Jr. et al. proposed a theoretical test structure consisting of a circular array of tightly spaced Schottky-barrier junctions with independent contacts. This setup formed a "bulls-eye" shaped target of many independent sensitive detectors that could be individually triggered, digitized, and logged as an incident energetic heavy ion entered the test structure and passed through. Simulations showed that the collected data could then be analyzed and the effective track profile extracted. In [5], Musseau et al. proposed and implemented a similar

Manuscript received July 19, 2004. This work was supported in part by DTRA.

Aaron S. Kobayashi is with Vanderbilt University, Nashville, TN 37237 USA (phone: 615-343-6705, e-mail: aaron.kobayashi@vanderbilt.edu).

Andrew L. Sternberg is with Vanderbilt University, Nashville, TN 37237 USA (phone: 615-343-6705, e-mail: andrew.l.sternberg@vanderbilt.edu)

Lloyd W. Massengill is with Vanderbilt University, Nashville, TN 37237 USA (phone: 615-343-6677, e-mail: lloyd.massengill@vanderbilt.edu)

Ronald D. Schrimpf is with Vanderbilt University, Nashville, TN 37237 USA (phone: 615-343-0507, e-mail: ron.schrimpf@vanderbilt.edu)

Robert A. Weller is with Vanderbilt University, Nashville, TN 37237 USA (phone: 615-343-6027, e-mail: robert.a.weller@vanderbilt.edu)

structure using multiple silicon microstrips separated by an insulated polysilicon trench as the sensitive detector.

In addition to the experimental approach, many analytical models [6, 7, 8] and computer codes [9, 10, 11] have been developed. The analytical model of [6] (Equation 1), based on the Rutherford formula for δ-ray distribution, has been widely used in determining the dose deposited in a cylindrical shell with radius *t* and thickness *dt.*

$$D(t) = \frac{Ne^4 Z^{*2}}{\alpha mc^2 \beta^2 t}\left[\frac{\left(1-\frac{t+\theta}{T+\theta}\right)^{1/\alpha}}{t+\theta}\right] \quad (1)$$

D(t) is the dose deposited in a cylindrical shell at a distance t from the track of an incident ion with an effective charge Z^* and relative velocity β through a medium containing N electrons per cm^3. The electron charge and mass are e and m respectively and c is the speed of light. The effective charge is defined in terms of the atomic number Z of the incident ion as follows [6]:

$$Z^* = Z(1 - e^{-125\beta \cdot Z^{-\frac{2}{3}}}) \quad (2)$$

The parameter θ defined by [6]:

$$\theta = k(0.010\,keV)^{1.079} \quad (3)$$

where $k=6x10^{-6}$ g cm^{-2} $keV^{-1.079}$. The parameter T is defined by [6]:

$$T = kW^{\alpha} \quad (4)$$

where the α here and in (1) is selected such that for $\beta < 0.03$, $\alpha = 1.079$ and for $\beta > 0.03$, $\alpha = 1.667$. W is the kinematically limited maximum delta-ray energy given by [6]:

$$W = \frac{2mc^2\beta^2}{1-\beta^2} \quad (5)$$

Subsequently, we express D(t) in units of $eV/\mu m^3$.

In device simulations, the radial distribution of charge generated by an ion strike is typically approximated by fitting a distribution function, typically Gaussian, around the center of an average track based on LET [12]. This procedure is theoretically and practically sound for larger devices, but for smaller ones, where the size of the device is not sufficient to average the track, the microstructure of the track is potentially extremely important.

Here we will investigate both the spatial and temporal evolution of energy deposited by proton and alpha strikes in silicon using a Monte Carlo approach based on Geant4 that treats continuous energy loss, discrete δ-rays, and nuclear reactions in a single consistent framework.

II. Simulation Details

A. Model Description

In real world experiments, the ion impact location can be considered random. A distinct advantage of a simulation based approach lies in the ability to precisely control the impact point of an ion. Fig. 1 shows graphical representations of the superposition of 1000 ion strikes by protons and α particles at the same location in Si. The incident ion tracks are straight and represent ions moving from the left to the right through the center of each diagram.

Surrounding the ion tracks in Fig. 1 are the highly segmented trajectories of large numbers of discrete secondary electrons, frequently called δ rays. These fast electrons are the agents by which the energy of the primary ions is distributed locally around the track. Apart from the greater density of δ rays produced by the α particles, the most striking feature of the figures, and particularly of the proton figure, is the extremely high degree of variability associated with these secondary particles.

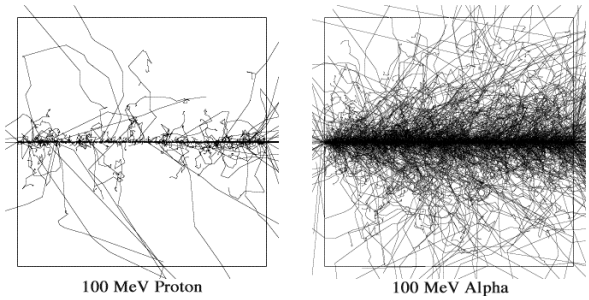

Fig. 1. An example simulation 1000 events in a 6 μm silicon cube. The simulation results including all secondary particles for 100 MeV protons are depicted on the left and for 100 MeV α particles on the right. Most significant are the large number of δ electrons surrounding the track. The greater ionization of the α particles is obvious in the density of these secondary particles.

δ rays are responsible not only for the intrinsic variability of LET, but also for the variability of the spatial distribution of energy. In both cases shown in Fig. 1, nuclear reactions in the volume of interest are absent. These infrequent events lead to much greater spatial and energetic variability than δ rays, and are included explicitly with the appropriate probability of occurrence in the results that follow.

Since ions and their secondary particles on average exhibit radial symmetry as they pass through silicon, a bulls-eye structure similar to the one described in [4] is a natural choice as a sensitive test volume. Our virtual detector is created with twenty concentric cylinders of geometrically increasing thickness from 1 nm to an outer radius of 5 μm.

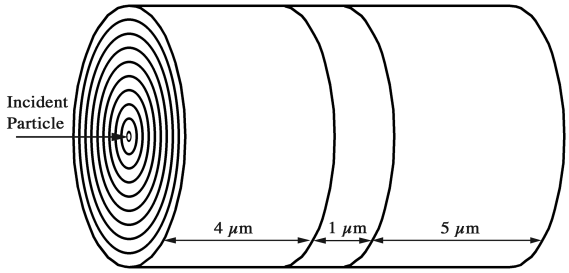

Fig. 2. Schematic of target detector in silicon. The detector is composed of twenty concentric cylindrical shells of geometrically increasing thickness, and divided into three layers with thicknesses as shown.

The resulting target is 10 μm thick and is divided into 4 μm, 1 μm, and 5 μm thick layers respectively (Fig. 2). The homogeneous target is divided in this fashion to create a center section in which energy can be separately tracked. Results from this "virtual" section can then be compared with

those from the front and back sections to quantify surface effects as well as cleanly estimate LET. In particular, the effects of the δ rays, many of which obviously originate from energy deposition in the thicker adjacent sections, on LET can be determined.

Geant4 version 4.6.0-p01 was used to build the application used for this work. Low energy electromagnetic physics was included, as well as a comprehensive set of hadrons and hadronic interactions, including the binary intra-nuclear cascade model from Geant4 to describe nuclear reaction events. The target was configurable at run time and could be any of a number of variations on a basic multilayer planar structure described above. The ion beam was always normally incident.

III. Results and Discussion

A. Complex Track Structures

One key advantage of this simulation technique is the ability to examine the complex track structure of incident particles in three dimensions. This level of detail allows us to demonstrate the extreme variability of events as well as examine the details of their geometrical structure. We will use this new information first to verify the average results of our simulations and then construct plots detailing the distribution of events in a selection of the concentric rings of the target structure.

B. Simulator Validation

In the following section, we compare our Geant4 simulations with previous works.

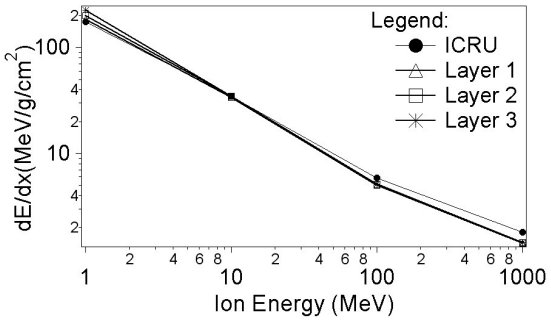

Fig. 3. The proton stopping power (dE/dx) in silicon for each test layer in the target.

The first test is a stopping power comparison. In Fig. 3 we have calculated *dE/dx* for proton energies in each of the three silicon target layers over an energy range of 1 MeV to 1 GeV and compared it with the ICRU [13] proton stopping power tables. The calculated LET shows satisfactory agreement over the depicted data range.

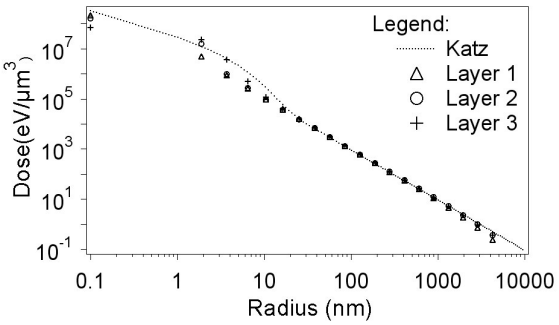

Fig. 4. The simulated dose as a function of radius for 100 MeV incident protons as compared to the analytical model of [7].

The second test compares the radial distribution of dose by a proton beam with the analytical model of Katz and collaborators. In Fig. 4 the mean density of energy deposited in the various annular rings depicted in Fig. 2 by 100 MeV protons is shown along with the corrected Katz analytical track model described by Waligorski et al. [7]. The energy of the central cylinder in Fig. 2, which is correctly associated with zero radius, is shown at 0.1 nm because Fig. 4 is a log-log graph. The electron density of water has been replaced by that of silicon as proposed by Fageeha [8]. Each of the three layers maintains good agreement over the large test range, indicating that for sufficiently energetic incident particles, there is negligible effect at the front and back surfaces of the target geometry.

It is important to stress that there are no adjustable parameters in Fig. 4. The mean density of deposited energy for a set of one billion particles has been computed by the analytical and Monte Carlo procedures separately and no normalization of the two curves has occurred.

C. Event Variability

Fig. 5 shows the calculated radial dose contributed by 100 MeV protons and alphas. The calculated energies include all energy generated by both primary and secondary particles in the silicon target in units of eV/μm^3 and the standard deviation of this dose. There are three lines for both the energy and standard deviation to represent the three layers that comprise the total volume of the target detector. The most striking result obtained from these curves is the very large size of the uncertainty values when compared with the values themselves. This result is consistent with the physical simulation depicted in Fig. 1. The high degree of variability is the result of extreme δ-ray and nuclear reaction events that, although rare, can deposit extremely large amounts of energy and charge. For example, the LET for the primary particle is less than 10 keV, but more than 3% of events deposit greater than 1 MeV in a target detector of this size.

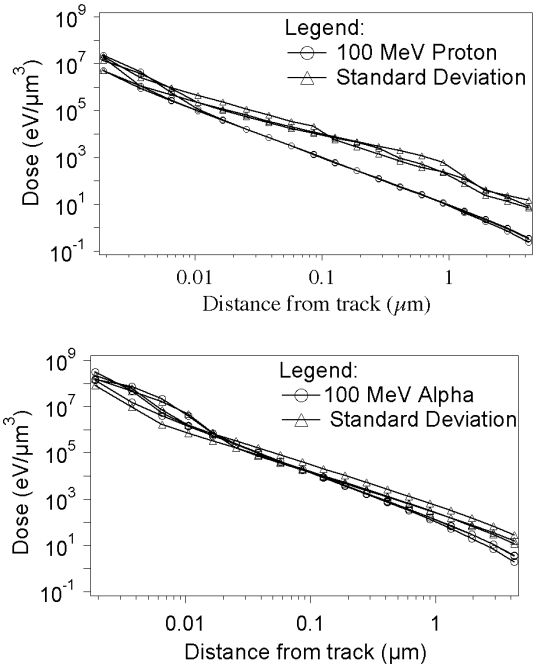

Fig. 5: The simulated radial dose as a function of radius compared to the standard deviation of the data.

Fig. 6 shows the radial deposition over five decades of incident proton energy in the same cylindrical silicon target. For high incident particle energies, the deposition maintains the power-law form seen in Fig. 4. However, below 10 MeV, the distribution begins to change shape and the deposition is no longer quite so similar in all three cylinders. The shape change is due to the diminished range of δ electrons that are produced by lower energy primary ions. Additionally, nuclear reactions, which are also responsible for the statistical broadening of tracks, diminish and eventually disappear for the lowest energy primary ions. Fig. 7 similarly shows the comparable radial distribution for incident α particles over four decades of energy beginning at 10 MeV.

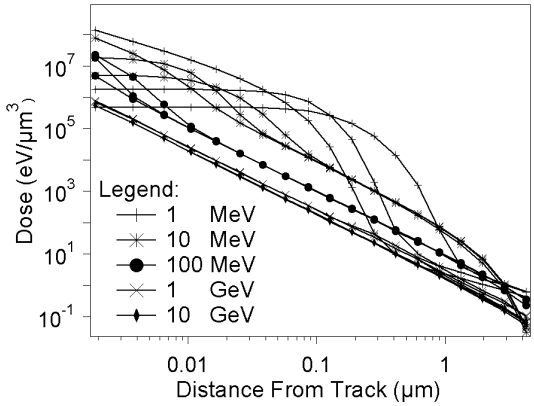

Fig. 6. The simulated dose by protons vs. distance from the track center for four decades of incident proton energy.

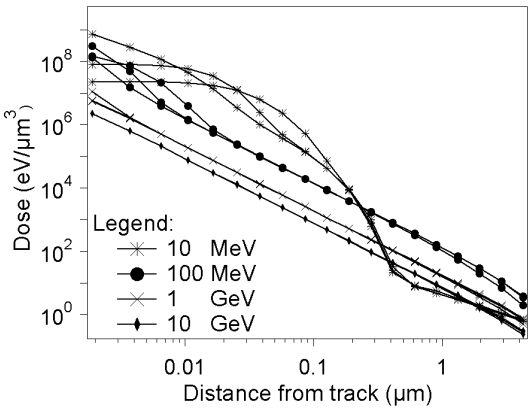

Fig. 7. The simulated dose by Alphas vs. distance from the track center for four decades of incident alpha energy.

D. Event Distributions

One of the key advantages of using a Monte Carlo code such as Geant4 is the ability to track and record the contributions of individual ions as they pass through the target material. By recording both the locations and energy depositions of all events, it is possible to compute the distributions of the energies in each shell of the target detector. Viewed in this way, one may interpret each point in Fig. 4 as being the mean of a distribution of possible energy values deposited in a given ring by a primary ion. These distributions are almost as readily accessible as the averages themselves and offer a fascinating insight into the variability of individual events.

For largely asymmetrical distributions such as those suggested in Fig. 5, the third and fourth moments of the distribution commonly referred to as skewness and kurtosis are commonly used for characterization. Our distributions are so variable in shape that they are not well characterized by such moments. We have chosen to deal directly with the distributions. Fig. 8 shows four of these event distributions for 100 MeV protons in rings 1 (0 nm), 5 (10.5 nm), 10 (85.6 nm), and 20 (4.3 μm), respectively. It is interesting to note that a very different distribution of events exists near the center of the track when compared with events at the edges of our target cylinder. Not surprisingly, there are a much larger number of events occurring in the core cylinder. For this core cylinder, a peak followed by a steep falloff occurs around an event that deposits 1 keV of energy. In ring 20, events are less common because either discrete δ rays or nuclear reaction products are generally needed to propagate energy to this distance. As the radial distance increases, events do not exhibit the same concentration about a specific energy value as seen in the core cylinder. However, the variability is very large with some events depositing in excess of 10 keV. Even allowing for the larger volume, this is a dramatic difference when compared to the 1 keV peak found in the core cylinder. Thus, while events are much less common at larger distances from the track, events that do reach this range are more likely to be highly energetic.

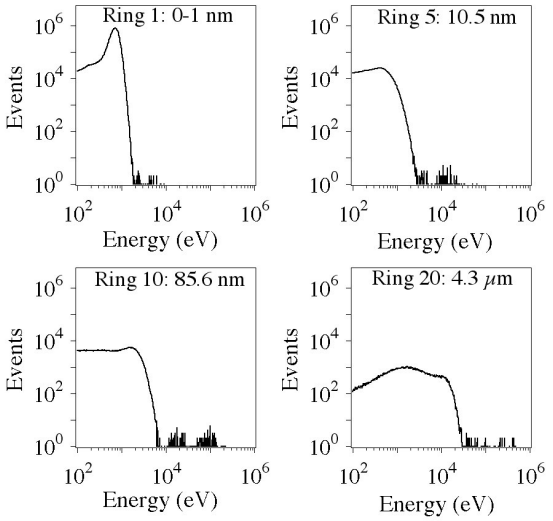

Fig. 8. The distribution of energetic events in layer 2 of the detector target as generated by 100 MeV protons.

E. Temporal Evolution

When modeling single events with microstructure it is still necessary for practical reasons to add charge in a device model in a way that avoids numerical instability. Thus, it is commonly assumed on the one hand that energy deposition by an energetic ion is instantaneous and on the other that the time evolution of the generation rate may be modeled as a narrow Gaussian. The machinery described above makes the study of complex radiation interactions in detail possible and thereby makes the quantification this assumption possible. Fig. 9 shows the dose as a function of time obtained from an analysis of 300 MeV protons incident on Si. An ensemble of 726 events with total deposited energy exceeding 50 keV was chosen from a run of 10^7 total events. This subset was selected because only the most energetic events will be candidates to cause single event upsets, and therefore only these will be simulated in detail.

Although the resulting curve appears regular in form, different temporal regions can be identified with different physical processes. The tail above approximately 0.2 ps is primarily the result of energetic recoiling residual nuclei. Spallation reactions limited to light reaction products characteristically were complete by about 0.2 ps, while the duration of δ-ray events was of order 0.1 ps. In [14], Oldiges et al. found that energy deposition occurred over a period of approximately 0.5 ps, a number in good agreement with our simulation results.

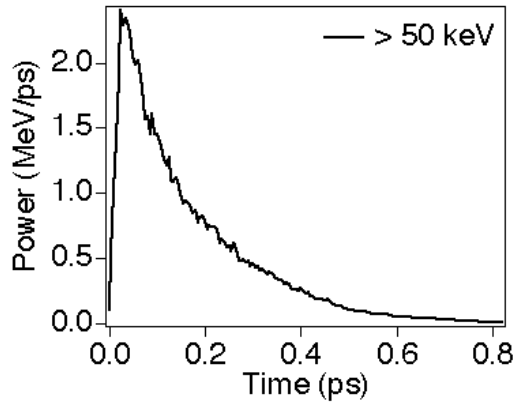

Fig. 9. Average power as a function of time for events depositing > 50 keV for 300 MeV protons incident on a 2.5 μm diameter cylinder of Si 5 μm thick.

Fig. 10 depicts the average power of 100 MeV α particles in a similar silicon target. The solid curve represents events that deposited greater than 50 keV of energy in the sensitive detector. More than 99% of the incident particles passed this criterion. Also show in Fig. 10 is the curve representing the average power as a function of time for events that deposited > 500 keV in the target. This criterion filtered out more than 99.9% of the 4 million simulated ion strikes resulting in approximately 30 candidate events. For the 50 keV case, the power is approximately constant during the time it takes for an incident alpha particle to traverse the detector. For the 500 keV case, it is dominated by the contributions of slower secondary particles.

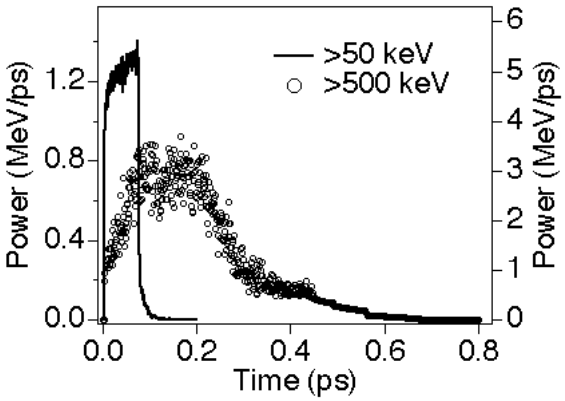

Fig. 10. Average power as a function of time for 100 MeV alpha particles incident on a 2.5 μm diameter cylinder of Si 5 μm thick. The solid curve (left axis) represents an average of events exceeding 50 keV of deposited energy. The other curve (right axis) represents an average of events exceeding 500 keV of deposited energy.

Importantly, Fig. 9 and Fig. 10 confirm that the physical approximation of instantaneous deposition is reasonable for these energetic incident particles, since the time over which the deposition occurs is significantly less than the response time of typical devices. In addition, the convolution of the Gaussian and exponential functions, which exists in closed form involving the error function, may be used for charge introduction in device simulators, where a Gaussian alone is now typically used by default.

IV. Conclusion

We have introduced a new Monte Carlo simulation technique based on Geant4 for obtaining detailed information about the track, spatial, and temporal characteristics of energetic proton and alpha particles in silicon to be used in support of a single-event prediction strategy based on averaging of ensembles extreme radiation events with physically correct microstructure. We have demonstrated that this approach yields average energy deposition in agreement with ICRU values and extended track structure in agreement with the model of Katz and collaborators, both without the use of adjustable parameters.

Extending the computations to the distribution of energy at various distances from an ion track has revealed the range of possible variation, particularly due to discrete δ rays and nuclear reaction fragments that may be expected when applying the analytical Katz model of track structure to the energy described by LET.

Finally, we have analyzed the temporal characteristics of the energy deposition in a target by a proton beam by accounting for energy deposited by the beam and all secondary particles individually. The results indicate that most energy is transferred to the target in approximately 0.1 ps and that even when nuclear reactions are involved, events are characteristically complete within approximately 1 ps.

In conclusion, these results confirm that ensembles of discrete radiation events generated with Geant4 reproduce average ion-strike properties, which agree quantitatively with established theory and data. The use of such ensembles, particularly those of extremely energetic δ ray and nuclear reaction events, to predict single event effects in specific devices will be the subject of forthcoming publications.

V. Acknowledgment

The authors acknowledge many useful and enjoyable discussions with D. M. Fleetwood and R. A. Reed in the continuing development of Geant4 for single event studies.

VI. References

[1] R.A. Weller, A.L. Sternberg, L.W. Massengill, R.D. Schrimpf, and D.M. Fleetwood, "Evaluating average and atypical response in radiation effects simulations," IEEE Trans. Nucl. Sci., vol. 50, No. 6, 2265-2271, Dec. 2003

[2] S. Agostinelli, et al., "Geant4 — a simulation toolkit," Nucl. Instr. and Methods in Physics Research A, Vol. 506, pp. 250-303, 2003.

[3] C. Inguimbert, S. Duzellier, and R. Ecoffet, "Contributions of GEANT4 to the determination of sensitive volumes in case of high-integrated RAMs," IEEE Trans. Nucl. Sci., vol. 49, no. 3, pp. 1480-1485, June 2002.

[4] J.W. Howard Jr., R.C. Block, W.J. Stapor, P.T. McDonald, A.R. Knudson, H. Dussault, and M.R. Pinto, "A novel approach for measuring the radial distribution of charge in a heavy-ion track," IEEE Trans. Nucl. Sci., Vol. 41, pp. 2077-2084, Dec. 1994

[5] O. Musseau, V. Ferlet-Cavrois, A.B. Campbell, A.R. Knudson, S.Buchner, B.Fisher, and M.Schlögl, "Technique to measure an ion track profile," IEEE Trans. Nucl. Sci., vol. 45, pp. 2563-2570, Dec. 1998

[6] Z. Chunxiang, D.E. Dunn, and R. Katz, "Radial distribution of dose and cross-sections for the inactivation of dry enzymes and viruses," Radiat. Protect. Dos., vol. 13, pp. 215-218, 1985.

[7] M.P.R. Waligorski, R.N. Hamm and R. Katz, "The radial distribution of dose around the path of a heavy ion in liquid water," Nucl. Tracks Radiat. Meas., vol. 11, No. 6, 1986.

[8] 0. Fageeha, J. Howard, and FL C. Block, "Distribution of radial energy deposition around the track of energetic charged particles in silicon," J. Appl. Phys., vol. 75, no. 5, pp. 2317-2321, Mar. 1994

[9] W.J. Stapor and P.T. McDonald, "Practical approach to ion track energy distribution," *J. Appl. Phys.*, vol. 64, no. 9, Nov. 1988.

[10] W.E. Wilson and Hooshang Nikjoo, "A Monte Carlo code for positive ion track simulation," *Radiat. Environ. Biophys.*, vol. 38, pp. 97-104, Feb. 1999

[11] A. Akkerman and J. Barak, "Ion-track structure and its effects in small size volumes of silicon," *IEEE Trans. Nucl. Sci.*, vol. 39, no. 6, pp. 1613-1621, Dec. 2002.

[12] "Dessis User Manual Release 9.5", ISE Integrated Systems Engineering, Zurich, Switzerland, Pg 275

[13] "Stopping Powers and Ranges for Protons and Alpha Particles," Int. Commission Radiation Units and Measurements, Bethesda, MD, vol. 49, 1992.

[14] P. Oldiges, R. Dennard, D. Heidel, Bill Klaasen, F. Assaderaghi, M. Ieong, "Theoretical Determination of Temporal and Spatial Structure of α-Particle Induced Electron-Hole Pair Generation in Silicon," *IEEE Trans. Nuc. Sci.*, vol. 47, no. 6, pp. 2575-2579, Dec 2003.